Near-interface sensing, imaging and nanometrology using smart surfaces.

Adi Salomon[1,2,3,*] and *Martin* Oheim[3,*]

[1] Chemistry department, Bar-Ilan University, 529000, Ramat-Gan, Israel ;
[2] Institute of Nanotechnology and Advanced Materials (BINA), Bar-Ilan University, 529000, Ramat-Gan, Israel ;
[3] Université Paris Cité, SPPIN, Saints-Pères Paris Institute for the Neurosciences, CNRS, Paris, France.

We present two distinct types of 'smart' surfaces designed for facilitating the quantitative exploration of dynamic processes occurring at sub-wavelength distances from interfaces, using far-field optical techniques. Based on evanescent waves in excitation and/or emission, we achieve an axial localization precision of about 10 nm. The first type of substrate incorporates nanocavities in a thin metallic film, enhancing and confining the electromagnetic field to a tiny volume. The second sample consists of a thin fluorescent film sandwiched between transparent spacer and capping layers deposited on a glass coverslip. The emission pattern from this film codes detailed information about the local fluorophore environment, namely, the refractive index, defects, reciprocal lattice, and the axial distance of the molecular emitter from the surface. An application to axial metrology in total internal reflection fluorescence and axial super-localisation microscopes is presented.

INTRODUCTION

Characterizing processes occurring at or near interfaces is paramount for understanding the chemical interactions on electrode surfaces or the dynamics occurring at or near the plasma membrane. Despite significant advances, many tools for surface characterisation with nm-resolution are often limited to vacuum conditions, making *in-situ* and *in-operando* experiments impossible. Optical methods on the other hand, offer more versatility and simpler sample handling but they lack surface selectivity and quantitative measurements are more difficult to realise than with electron microscopy.

Here, we introduce two different types of innovative 'smart' surfaces that we designed for the study of dynamic processes at sub-wavelength distances from a glass substrate, using far-field optics. The first type of 'smart' surface consists of nanocavities etched into metallic thin films. In these plasmonic samples, the electromagnetic (EM) field is amplified in specific hot-spots and thereby confined to a sub-wavelength volume [1], **Fig.1a**. The second type of surface features a homogeneous fluorescent thin film [2-4], the emission pattern from which probes the local fluorophore environment. Both surfaces have in common that they rely on the excitation or detection, respectively, of evanescent waves through a high-NA objective. Our smart surfaces reveal information regarding the refractive index (RI) [3], the axial fluorophore height (along z, the microscope's axis) [3,4] and molecular orientation, via the analysis of the radiation patterns of near-surface emitters [3-6].

Experimental details

Plasmonic meta-surfaces were produced by milling sub-wavelength cavities into a flat silver film. As a result of the structured surface, Bragg scattering creates the conditions for k-vector matching, so that propagating light can couple to plasmonic modes, leading to the formation of hot-spots at the surface. The cavity pattern can be designed so that the EM field is confined onto the smooth surface, *between* the cavities, which removes the necessity of depositing the analyte inside the cavity. The frequency of the enhanced EM field depends on the structure, the RI of the medium in contact, the precise type of metal and the polarisation state of the driving EM field. With such metallic structures we could detect trace amounts of molecules deposited onto the interface with a sensitivity of 10^{-10} M [8].

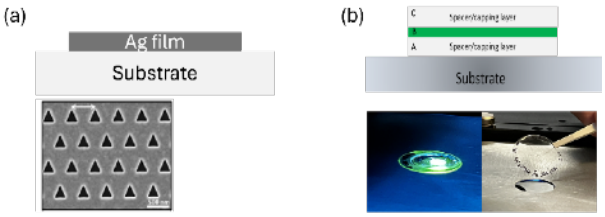

Fig.1. *Two types of smart surfaces.* (a), nanocavities milled into a thin silver film. *top,* schematic cross section, *bottom*, scanning electron microscope (SEM) image of a nano-fabricated triangular hole array. (b), fluorescent thin film sandwich, *top*, in which the distance of the fluorescent layer from the glass is controlled by the thickness of a transparent spacer thin film having the RI of a cell (1.34) and the ensemble is sealed with a transparent, index-matched polymer. *Bottom*, the resulting films are brightly fluorescent and perfectly transparent.

* Corresponding authors: adi.salomon@biu.ac.il, martin.oheim@u-paris.fr

For the fluorescent thin films, we developed a new class of nanoscale emitters. Unlike single-molecule deposits, crystalline or spin-coated dye layers, or even quantum dot layers, our 8-nm thin films are composed of biocompatible hydrogel nano-beads as building blocks. Many different fluorescent molecules can be chemically attached to these beads to form nanobead emitters (NBEs), not only uncoupling the surface chemistry and dye chemistry, but also creating a versatile toolbox for surface fluorescence microscopy and spectroscopy. In fact, the same dye molecules can be used for metrology and for the chemical or biological experiment.

The NBEs are deposited using a modified layer-by-layer (LBL) technique, resulting in a transparent and well-defined film, with bright fluorescence and - for most dyes studied - the same spectrum as the solution, **Fig. 1b**.

Calibrating evanescent-wave penetration depth

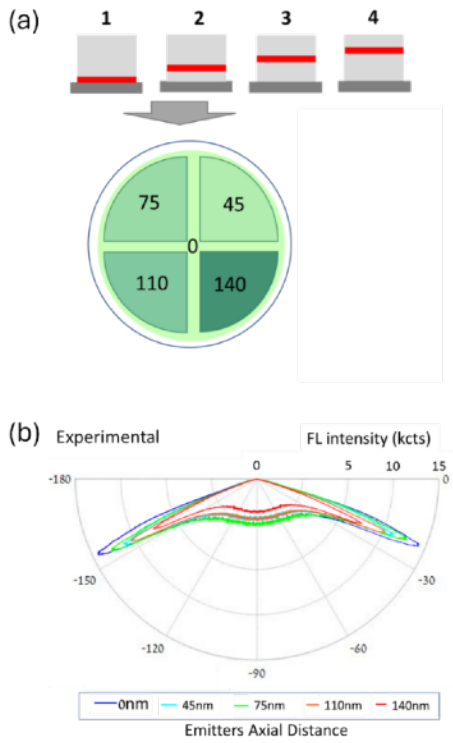

Fig.2 *EW calibration.* (a), sketch of a series of thin-film samples. A flat, homogeneous fluorescent layer is deposited at 0, 45, 75, 110, and 140-nm distance from the glass substrate, embedded in a transparent spacer of RI = 1,33. (b), polar plots of the measured emission pattern of the above samples. The closer the emitter is to the surface, the brighter it is and the more it emits to supercritical angles.

This second type of sample is a powerful tool for the calibration of the evanescent-wave (EW) penetration depths in total internal reflection fluorescence (TIRF) microscopy, a long-standing metrology problem. TIRF in principle allows for the precise axial localisation of fluorescent molecules or organelles [5] close to a glass substrate. However, the quantitative interpretation of TIRF images is difficult, and it requires a precise knowledge of the shape of the EW decay, and test samples that closely mimic the biological specimen are required. Such samples should possess a well-defined fluorophore distribution so as to correlate measured intensities with axial fluorophore distances [7]. For such a sample to be useful, add criteria as spatial uniformity, minimal autofluorescence and stability over time.

Fig. 2 shows an example of how our nanometric axial rulers work for EW calibration: We produced a series of fluorescence thin films embedded in a medium having a RI of 1.34, and featuring different fluorophore heights between 0 and 140 nm above the interface. The measured fluorescence intensities decayed exponentially as a function of axial distance, and the corresponding radiation patterns measured on backfocal plane (BFP) images showed the expected distance-dependent change, with less and less fluorescence emitted into supercritical angles upon increasing distance [3,7].

k-space imaging of silver nanostructures

Both types of surfaces can be combined when overlaying a structured nanohole array in silver with a thin, homogenous fluorophore layer. The BFP image collected from such a 'hybrid' sample contains a wealth of information, from the incidence plane and angle of the laser over structural parameters to the emitted fluorescence and excited plasmons.

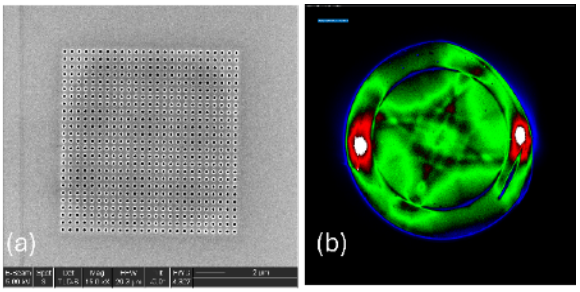

Fig 3. (a) SEM image of a square circular hole array with a cubic symmetry covered with a fluorescence thin film (TPPS J-aggregate). (b) Pseudocolour BFP image. The Brillouin zones are clearly observed in the under critical part of the BFP image (centre). The red/white spots in the periphery are the in and out laser beam suffering total reflection, and the sharp line on the right is the propagation direction of the surface plasmons.

References

1. A. Weissman, et al. Adv Opt Mater **5**(10), 1700097 (2017)
2. A. Weissman, *et al.*, Langmuir, **36**, 844 (2020)
3. H. Klimovsky, *et al.*, Adv Opt Mater **11**, 2203080, (2023)
4. I. Olevsko et al. Opt Commun, 130538 (2024) *in press*
5. M. Oheim, A. Salomon, M. Brunstein, Biophys J **118**, 2339 (2020)
6. M Brunstein, A. Salomon, M. Oheim ACS nano **12**(12), 11725-11730 (2018)
7. M Oheim, A Salomon US Patent 11,644,422; EU Patent EP18306193.6A (2019)
8. M. Hamode, et al. Environmental Science: Nano (2024) DOI: 10.1039/D3EN00821E *in press.*